Energy-based seismic design of structures with buckling-restrained braces

Jinkoo Kim† and Hyunhoon Choi‡

Department of Architectural Engineering, Sungkyunkwan University, Suwon, Korea

Lan Chung‡†

Department of Architectural Engineering, Dankook University, Seoul, Korea

Abstract. A simplified seismic design procedure for steel structures with buckling-restrained braces (BRB) was proposed based on the energy balance concept and the equal energy assumption. The input seismic energy was estimated from a design spectrum, and the elastic and hysteretic energy were computed using energy balance concept. The size of braces was determined so that the hysteretic energy demand was equal to the hysteretic energy dissipated by the BRB. The validity of using equivalent single-degree-of-freedom systems to estimate seismic input and hysteretic energy demand in multi story structures with BRB was investigated through time-history analysis. The story-wise distribution pattern of hysteretic energy demands was also obtained and was applied in the design process. According to analysis results, the maximum displacements of the 3-story structure designed in accordance with the proposed procedure generally coincided with the target displacements on the conservative side. The maximum displacements of the 6- and 8-story structures, however, turned out to be somewhat smaller than the target values due to the participation of higher vibration modes.

Key words: seismic design; buckling restrained braces; energy-balance concept; equal energy concept.

1. Introduction

The structural damage caused by earthquake ground motions results not only from the maximum response but also from the accumulated plastic deformation. However current seismic design practice, which account only for the maximum earthquake load and the maximum displacement, does not provide enough information on the inelastic behavior of the structure.

In this regard the energy-based seismic design method, which utilizes hysteretic energy of a structure as a main design parameter, is considered as a potential alternative to the conventional strength-based seismic design method. The method is more advanced in that the accumulation of earthquake-induced damage can be taken into account in the design procedure. Associated with energy-based seismic design, Riddell and Garcia (2001) presented a procedure for construction of hysteretic energy demand

spectrum. Uang and Bertero (1988) and Estes and Anderson (2002) obtained story-wise distribution of hysteretic energy in multi-story structures. Léger and Dussault (1992) investigated the effect of damping devices on the energy dissipation of structures. Akbas *et al*. (2001) proposed a design procedure in which the seismic input energy demand is dissipated by the accumulated plastic deformation at beam ends. Leelataviwat *et al*. (2002) proposed a seismic design method based on the energy balance concept. Chou and Uang (2002) proposed a procedure to compute the total energy demand and to distribute it along the height of structures using inelastic energy spectra. Those studies mentioned above were carried out for moment-resisting framed structures.

In this study the energy balance concept of Leelataviwat *et al*. (2002) is further extended to develop a simplified seismic design procedure for steel frames with buckling-restrained braces. As the design procedure utilizes the equivalent single degree of freedom (SDOF) system to estimate the input and the hysteretic energy demands, the seismic energy demands obtained in multi-story structures are compared with those of corresponding equivalent SDOF structures. Sixty earthquake excitations, recorded in three different soil conditions and used in SAC steel project (Somerville *et al*. 1997), are used to compute the seismic energy demands of multi-story and equivalent SDOF structures. For design of buckling-restrained braces (BRB), the design spectrum presented in UBC-97 is used to obtain seismic input and plastic energy. The validity of the design procedure is checked by nonlinear dynamic analysis with 7 earthquake records generated from the design spectrum.

2. Characteristics of buckling-restrained braced frames

The excessive lateral deformability of a steel moment-resisting frame can lead to excessive non-structural damage under moderate earthquakes. The lateral stiffness of an unbraced moment frame can be increased by diagonal braces; however the inelastic behavior of such a system may not be satisfactory because the cyclic behavior of braces results in significant degradation of stiffness and strength, and thus of energy dissipation capability, due to the global instability of the brace.

The energy dissipation capacity of a steel moment frame can be greatly enhanced by employing buckling-restrained braces. BRB usually consists of a steel core undergoing significant inelastic deformation when subjected to strong earthquake loads and a casing for restraining global and local buckling of the core element. According to previous experimental research (Saeki *et al*. 1995, Tremblay *et al*. 1999, Huang *et al*. 2000), BRB exhibits stable hysteretic behavior and high energy dissipation capacity. Iwata *et al*. (2000) showed that BRB with yield stress of 262 MPa behaved stably when they were stressed more than 3% of strain, which corresponds to ductility ratio of 24. Similar results were obtained by Black *et al*. (2002) who showed that a structure with buckling restrained braces with yield stress around 280 MPa behaved stably at 3% of inter-story drift. The ductility ratio at this point reached 20. Yamaguchi, *et al*. (2000) carried out experiments of half frames with buckling-restrained braces made of low-strength steel (F_y=96 MPa). Although not shown specifically in a table, it can be observed in the figure that the maximum ductility ratio reached as high as 30. Based on the experimental findings, it can be concluded that BRB has enough ductility to dissipate large amount of hysteretic energy.

Recommended provisions have been developed in draft form for design, detailing and testing of BRB based on current strength design philosophy by a joint AISC-SEAOC Task Group (SEAOC 2001). Currently, the design procedure generally applied for the buckling-restrained braced frames is similar to that used for special concentrically braced frames. Further research is still required for development of system level design procedure to apply BRB as a powerful and economic alternative of seismic design.
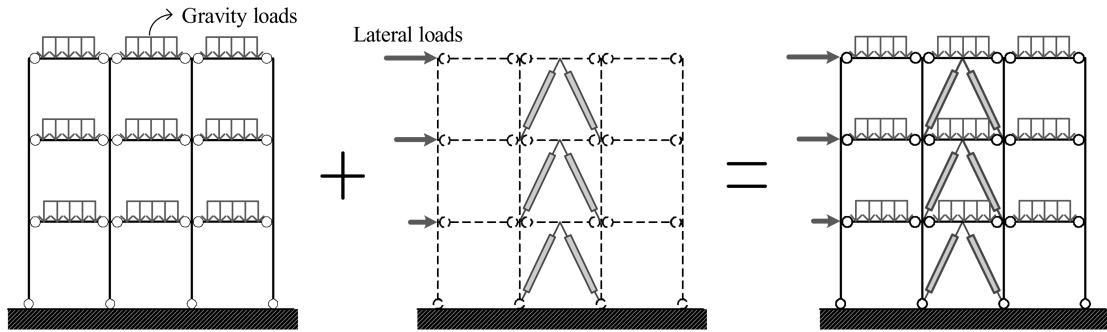
Fig. 1 Schematic of a buckling-restrained braced frame with hinged connections

Fig. 1 shows the schematic of a structure with BRB, in which the beams and columns are designed to remain elastic under the earthquake load and the BRB are designed to dissipate all the input energy. As energy dissipation and the resultant damage are concentrated on braces, the demand for inelastic deformation and the damage in the main structural members are reduced significantly. The structure system has advantage in maintenance since the damaged braces can easily be replaced with new ones after damaged by major earthquakes.

3. Energy-based design procedure

3.1. Energy-balance concept

The energy balance concept is based on the assumption that the energy required to push a structure monotonically up to a target displacement is equal to the maximum earthquake input energy of an equivalent elastic system computed from pseudo-velocity of an elastic response spectrum (Leelataviwat *et al.* 2002). This simplifying approach provides a convenient tool for determining the seismic energy demand of a structure without carrying out time-history analysis. This is advantageous especially in preliminary design stage, since estimating exact amount of energy demand requires pre-determined structural properties as well as nonlinear time-history analysis with a specific ground motion.

Based on the energy-balance concept, the input seismic energy E_i per unit mass can be estimated as:

$$\frac{E_i}{M} = \frac{1}{2}S_v^2 = \frac{1}{2}\left(\frac{S_a}{\omega_n}\right)^2 \tag{1}$$

where M is the mass, S_v and S_a are the pseudo-velocity and pseudo-acceleration, respectively, and ω_n is the fundamental natural frequency. The energy balance concept stipulates that this input energy is equal to the stored energy of an equivalent elastic system, which is composed of the elastic energy E_e and the plastic energy E_p in the original elasto-plastic system, as shown in Fig. 2. The input energy, elastic energy, and the plastic energy can be expressed as follows:

$$E_e = \frac{1}{2}u_y V_y = \frac{1}{2}\frac{V_y^2}{M\omega_n^2}; \qquad E_p = V_y(u_m - u_y) \tag{2}$$

where u_y and u_m are yield displacement and the maximum displacement of a structure, respectively.
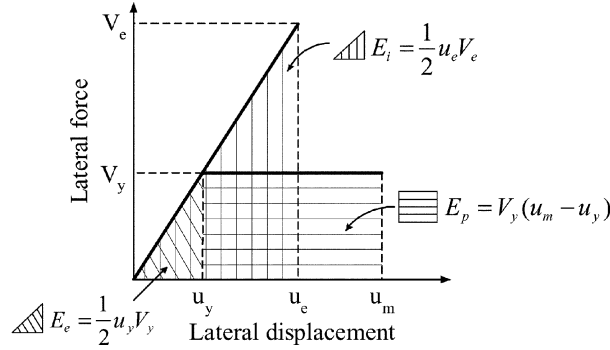
Fig. 2 Force-displacement relationship of a structure and an equivalent elastic system

By substituting target displacement u_T for the maximum displacement u_m, the above equation can be expressed as follows

$$E_i = \frac{1}{2}u_yV_y + V_y(u_T - u_y) \tag{3}$$

By substituting Eq. (1) for the input energy, the yield base shear, V_y, of a system which deforms to the target displacement when it is subjected to a specified seismic motion, can be computed from the above equation. Then the plastic energy per unit mass to be dissipated by BRB can be obtained by subtracting the elastic energy from the input energy:

$$\frac{E_p}{M} = \frac{E_i - E_e}{M} = \frac{1}{2\omega_n^2}\left\{S_a^2 - \left(\frac{V_y}{M}\right)^2\right\} \tag{4}$$

In this equation the damping energy is not included because it is already considered in the input energy.

3.2. Plastic energy in BRB

If a BRB is placed as a diagonal member with the slope θ as shown in Fig. 3, the energy dissipated by the BRB can be expressed as Eq. (5). The plastic energy (E_{pb}) in BRB when it is deformed to the maximum displacement corresponds to the area of the hatched rectangle in Fig. 4:

$$E_{pb} = F_{by}'\,(u_{bm} - u_{by}') = A_b\sigma_{by}\cos\theta\left(u_{bm} - \frac{L_b\sigma_{by}}{E_b\cos\theta}\right) \tag{5}$$

where F_{by}' is the yield force ($=F_{by}\cos\theta=A_b\sigma_{by}\cos\theta$), u_{by}', A_b, L_b, and θ are the lateral yield displacement ($=\dfrac{u_{by}}{\cos\theta} = \dfrac{1}{\cos\theta}\dfrac{L_b}{E_b}\sigma_{by}$), cross-sectional area, length, and slope of the BRB, respectively, and E_b is the elastic modulus of the brace. In the derivation of the above equation it is assumed that the BRB has elastic-perfectly plastic force-deformation relationship.
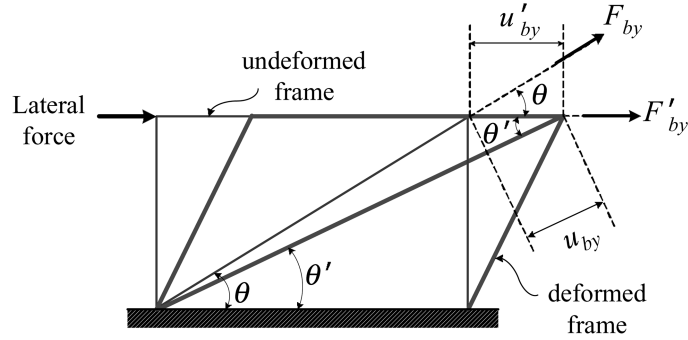
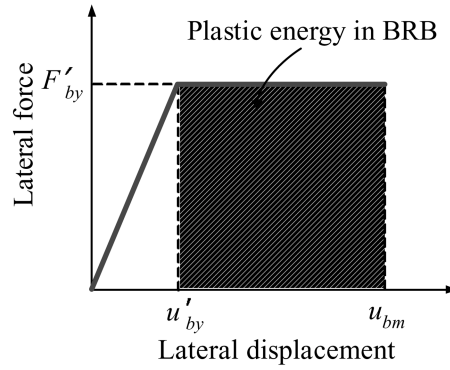Fig. 3 Deformed configuration of buckling-restrained braced frame

Fig. 4 Plastic energy stored in BRB

3.3. Design procedure for multi-story structures with BRB

The following procedure is followed to design a structure with BRB to meet a given target displacement. For simplicity, it is assumed that the seismic energy is dissipated solely by BRB, which can be realized practically by connecting beams and columns by hinges. Beams and columns are designed to resist gravity load plus the load induced from the braces, so that they remain elastic during the design-level earthquake.

Step 1. Determination of yield displacement and the target displacement

The yield displacement in each story of the proposed system can be derived as follows with geometry and yield stress of BRB (Fig. 3):

$$u_{yi} = \frac{\sigma_{byi} L_{bi}}{E_b \cos \theta_i} \tag{6}$$

where σ_{byi}, L_{bi}, and θ_i are the yield stress, length, and the slope of the brace in the ith story, respectively. If the story heights and the yield stress of braces are the same throughout the stories, the maximum displacement of the structure at yield, u_y, is the story yield displacement, Eq. (6), multiplied by the number of stories, N:

$$u_y = \sum_{i=1}^{N} u_{yi} = \frac{\sigma_{by} L_b}{E_b \cos\theta} \times N \tag{7}$$

Note that the yield displacement of the system does not depend on the cross-sectional area of the brace, and thus the yield displacement can be computed before the size of braces is finalized. The target displacement, u_T, is determined so that the given performance objective is satisfied.

Step 2. Conversion into an equivalent SDOF system

To apply the energy balance concept, the yield displacement and the target displacement of the original multi-story structure need to be converted into the corresponding values of the equivalent SDOF structure, u_y' and u_T', respectively, using the following relation (ATC 1996):

$$u_y' = \frac{u_y}{\Gamma_1 \phi_{t1}} \qquad u_T' = \frac{u_T}{\Gamma_1 \phi_{t1}} \tag{8}$$

where ϕ_{t1} is the coefficient of the fundamental mode shape vector corresponding to the roof story and Γ_1 is the modal participation factor. In the first stage, the fundamental mode shape can be assumed as linear. Also the effective mass participating in the fundamental mode of vibration is computed as follows:

$$M^* = \frac{\left(\sum_{j=1}^{N} m_j \phi_{j1} \right)^2}{\sum_{j=1}^{N} m_j \phi_{j1}^2} \tag{9}$$

Step 3. Estimation of natural period and input energy (E_i)

The pseudo-acceleration S_a is obtained from a design or a response spectrum using the fundamental natural period, T, and the seismic input energy can be estimated from Eq. (1). In the first stage of design the natural period needs to be assumed, then is computed more rigorously using an eigenvalue analysis once the first trial value for BRB size is determined. The natural period of the two-dimensional pin-connected braced frames is usually larger than that of the ordinary three-dimensional structures. In this study the first trial values for the natural periods of the model structures were computed using the IBC-2000 (International code council 2000) formula for concentric braced frame multiplied by 1.5:

$$T = 1.5 \times (0.049 h^{3/4}) \tag{10}$$

Step 4. Estimation of the yield base shear (V_y) and the plastic energy

The yield base shear V_y is computed from Eq. (3) and is substituted into Eq. (4) to obtain the plastic energy to be dissipated by BRB.

Step 5. Story-wise distribution of plastic energy

The plastic energy E_p obtained above should be properly distributed throughout the stories so that the plastic deformation in BRB is not concentrated in a few stories and the performance of each brace is maximized. Generally a linear story-wise distribution pattern is used as a distribution pattern for

simplicity; however in this study the story-wise hysteretic energy demands identified from time-history analyses of model structures using 20 earthquake records (Fig. 9) were used as energy distribution patterns.

Step 6. Determination of cross-sectional area of BRB (A_{bi})

The cross-sectional area of BRB required in each story to dissipate the specified input energy is obtained by equating the plastic energy obtained in Step 5 to the plastic energy in BRB when it is deformed to the target displacement u_T:

$$E_{pi} = F_{byi}(u_T - u_{yi}) = A_{bi}\sigma_{by}\cos\theta_i\left(u_T - \frac{L_{bi}\sigma_{by}}{E_b\cos\theta_i}\right) \tag{11a}$$

$$A_{bi} = \frac{E_{pi}}{\sigma_{by}\cos\theta_i\left(u_T - \frac{L_{bi}\sigma_{by}}{E_b\cos\theta_i}\right)} \tag{11b}$$

where E_{pi} is the plastic energy distributed to the ith story, F_{byi} is the story yield force, A_{bi}, L_{bi}, and θ_i are the cross-sectional area, length, and slope of BRB located in the ith story, respectively.

Step 7. Refinement of design

The first trial values for the plastic energy and BRB size are obtained based on the assumed natural period and the mode shape vector, and now more accurate values for these quantities can be obtained by eigenvalue analysis using the first trial size of BRB. The size of BRB is refined using the newly obtained natural period and mode shape vector, and this process is repeated until convergence.

4. Validity of the equivalent SDOF system

Large part of previous research on energy-based seismic design utilized the equivalent SDOF systems for estimating input and dissipated energies. However the validity of such an approach for structures with BRB needs to be verified.

4.1. Conversion into an equivalent SDOF system

Multi-story structures can be transformed into an equivalent SDOF structures using the base shear (V_b) - roof displacement (Δ_t) relationship obtained from pushover analysis. The story force for pushover analysis can be determined proportional to the design story force expressed as follows:

$$F_i = \frac{m_i\phi_{i1}}{\sum m_i\phi_{i1}}V_b \tag{12}$$

where F_i, m_i, ϕ_{i1}, and V_b are the story force at the ith story, mass of the ith story, and the design base shear, respectively. The base shear-displacement relationship of an equivalent SDOF structure can be obtained as follows

$$S_f = \frac{V_b}{M_1^*} \qquad S_d = \frac{\Delta_t}{\Gamma_1 \phi_{t1}} \tag{13}$$

where M_1^* and Γ_1 are the effective mass and modal participation factor.

4.2. Model structures and earthquake records for analysis

The three-bay 3-, 8-, and 20-story framed structures with BRB were prepared for analysis. The bay length of each model structure is 7.3 m, the height of the story is 5.5 m in the first story and is 3.7 m in the other stories. The weight of each story is 156.8 tonf and the inherent modal damping ratios are assumed to be 5% of the critical damping. The member cross-sectional dimensions and the modal properties of the model structures are presented in Fig. 5 and Table 1, respectively. The braces were designed for the equivalent static seismic load computed in accordance with UBC-97 with the seismic
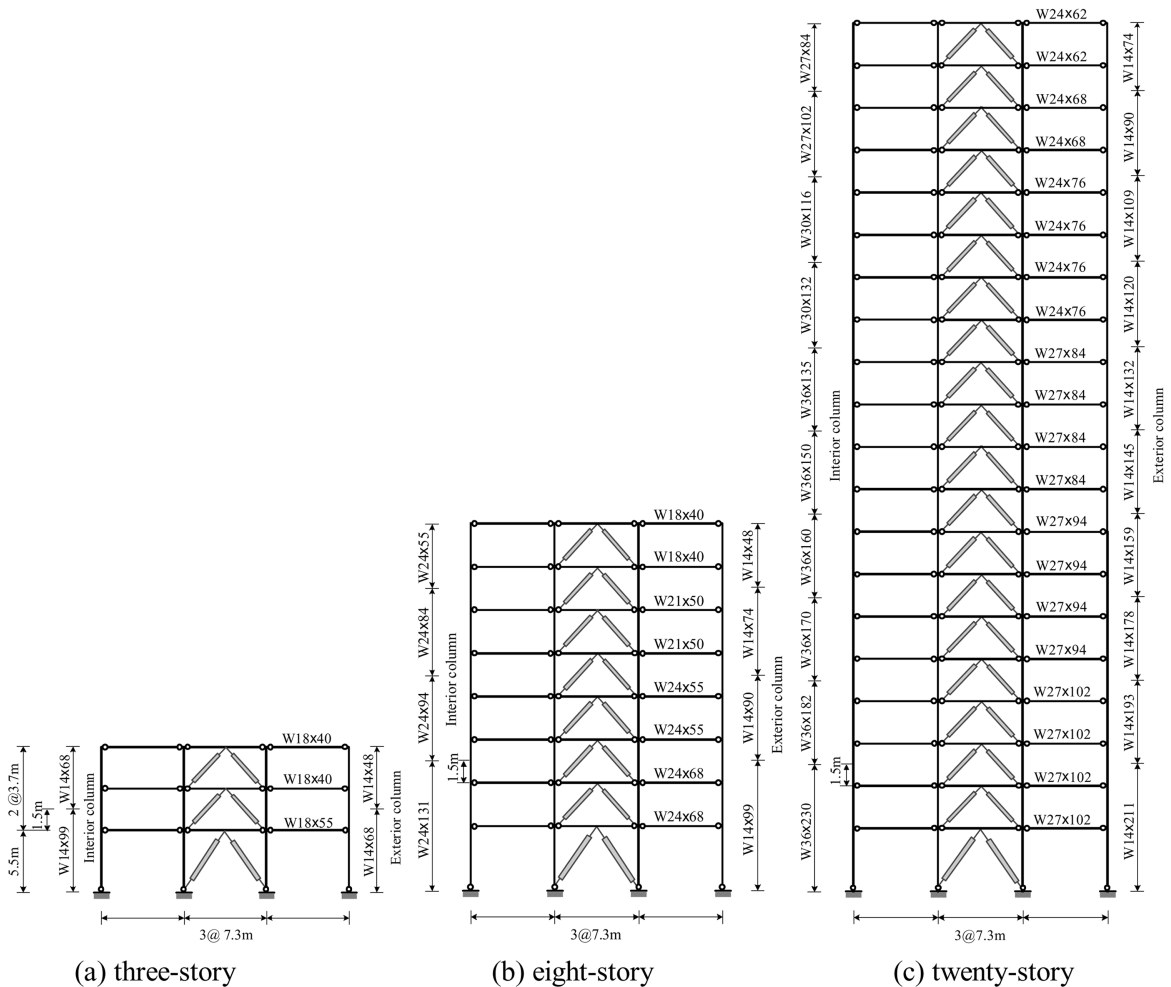

(a) three-story   (b) eight-story   (c) twenty-story

Fig. 5 Geometry of model structures

Table 1 Dynamic characteristic of model structures

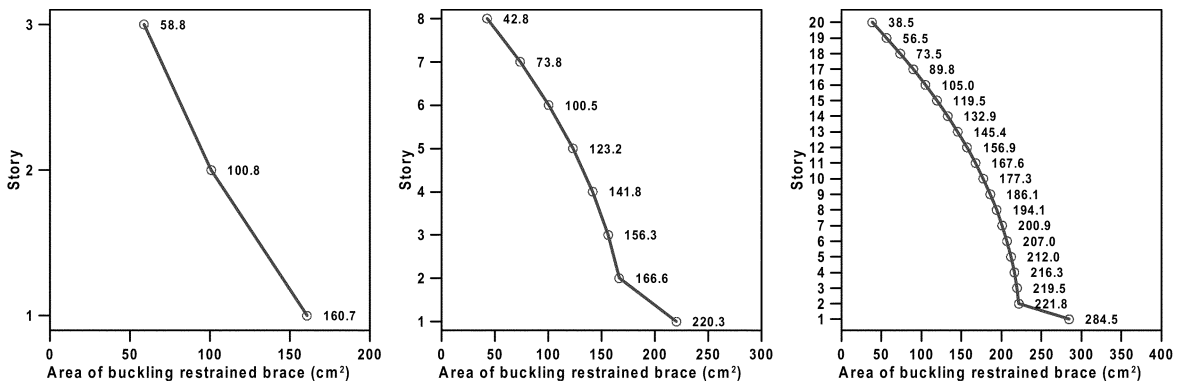| Structure type		3 story	8 story	20 story
Period (sec)	1st mode	0.463	1.077	3.972
	2nd mode	0.159	0.380	1.010
Effective modal mass (%)	1st mode	88.7	77.9	66.3

Fig. 6 The initial values for the cross-sectional area of buckling restrained braces

coefficients C_a and C_v equal to 0.4. Beams and columns were designed in such a way that they remain elastic for gravity load and the forces induced by the earthquake load. Fig. 6 presents the initial values for the cross-sectional area of BRB installed in each model structure. It was assumed that the force-axial deformation relationship of BRB was bilinear both in tension and compression with zero post-yield stiffness.

The earthquake ground excitations used in the analysis were taken from SAC steel project (Somerville *et al.* 1997), which presents 20 records for each of the soft rock, soft soil, and the near fault condition. The response spectra plotted in Fig. 7 show that earthquake records have quite different frequency contents.

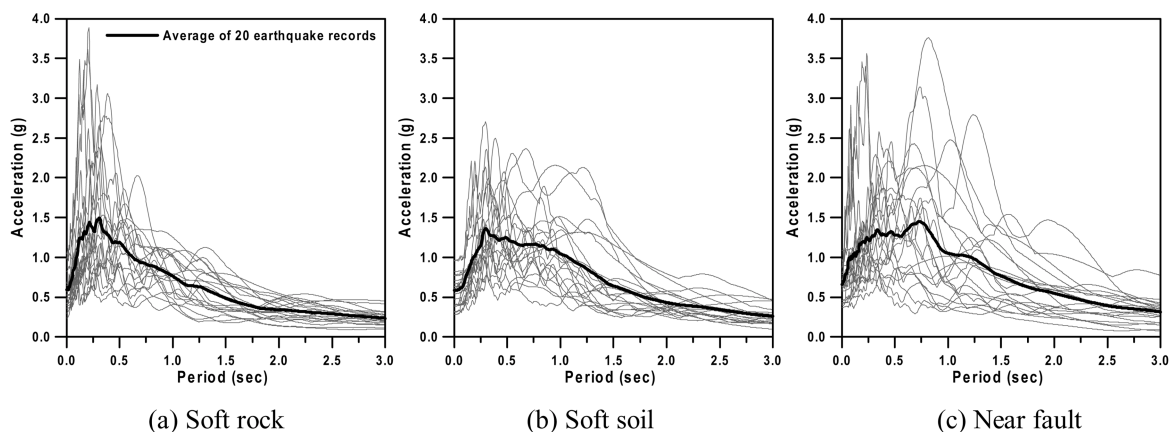(a) Soft rock   (b) Soft soil   (c) Near fault

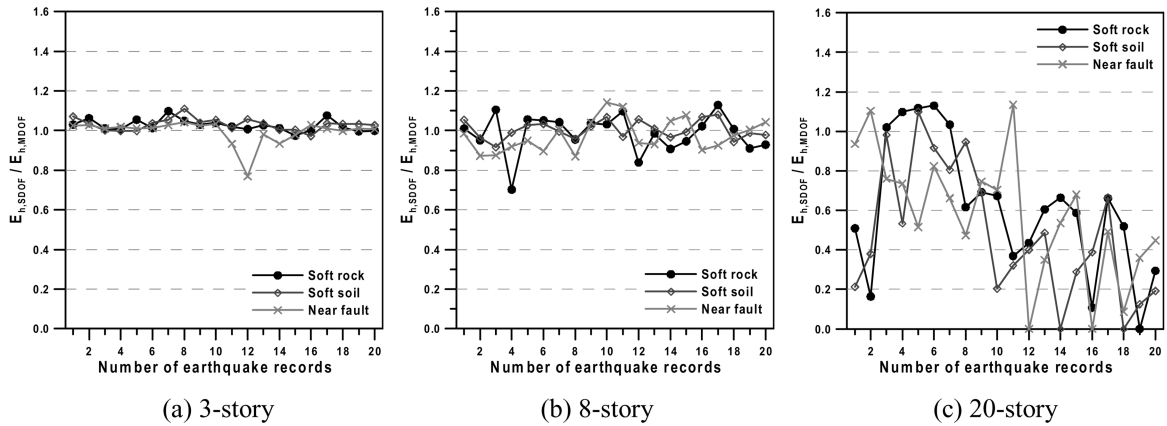Fig. 7 Response spectra of earthquakes recorded in different soil conditions

Fig. 8 Ratio of hysteretic energy in equivalent SDOF and MDOF structures

4.3. Comparison of results

The seismic input energy and the hysteretic energy demands in the original model structures and in the equivalent SDOF systems were computed. Nonlinear time-history analyses were carried out using the program code DRAIN-2D+ (Tsai and Li 1997). Fig. 8 illustrates the ratio of hysteretic energy demands in model structures to those of equivalent SDOF structures. It can be observed that in the 3- and 8-story model structures the energy demands obtained using the equivalent SDOF systems are compatible with those obtained using the original model structures, whereas those in 20-story structures are different significantly. The strong participation of higher modes may be the major reason for the inconsistency. No distinct difference could be observed for the three different soil conditions.

5. Application of the energy-based design procedure

5.1. Model structures and earthquake loads

Due to the large discrepancy in input and hysteretic energy between the results of original structure and the equivalent SDOF system of the 20-story structure, the design application was limited to lower story structures of 3-, 6-, and 8-story structures. The member sizes of 3- and 8-story structures are the same with those presented previously, and those of the 6-story structure are shown in Table 2.

5.2. Story-wise energy distribution and modification factors for equivalent SDOF system

Estes and Anderson (2002) found that the hysteretic energy demand in each story of steel moment frames is largest in the first story and decreases linearly in higher stories. Akbas *et al*. (2001) assumed linear distribution of hysteretic energy in energy-based design of steel frames. In this study the story-wise distribution patterns for hysteretic energy in structures with BRB were obtained through nonlinear time-history analyses using the previously used 20 earthquakes recorded in soft rock sites (Fig. 7(a)). Fig. 9 presents the hysteretic energy demands in each story of the model structures. In all cases the energy demand is largest in the first story and decreases with increasing height. The results for the story-wise distribution pattern of hysteretic energy demand were used in the design procedure.

Table 2. Properties of the 6-story model structure

Story	Column		Beam
	Interior	Exterior	
6	W 24×55	W 14×48	W 18×40
5			
4	W 24×84	W 14×74	
3			W 21×50
2	W 24×94	W 14×90	
1			W 24×55

(a) 3-story   (b) 6-story   (c) 8-story
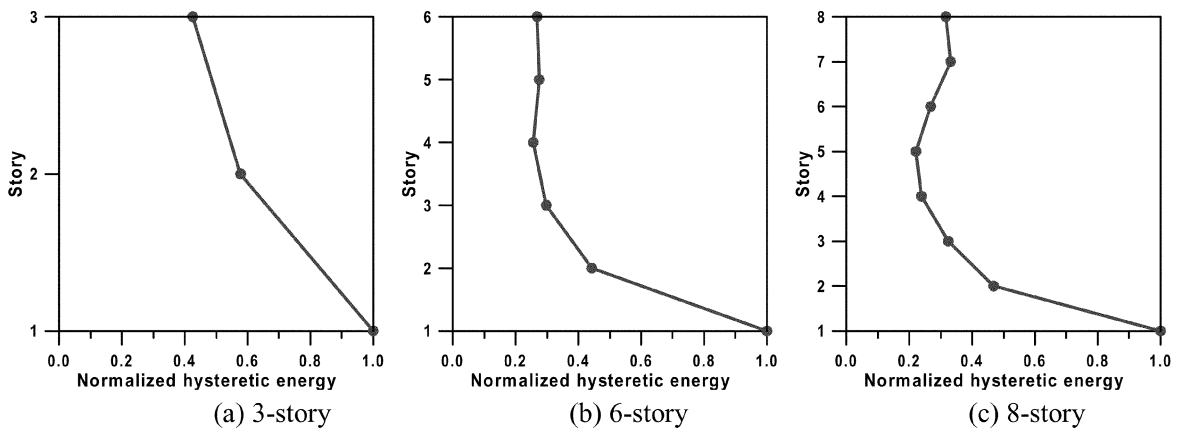
Fig. 9 Hysteretic energy demand in model structures
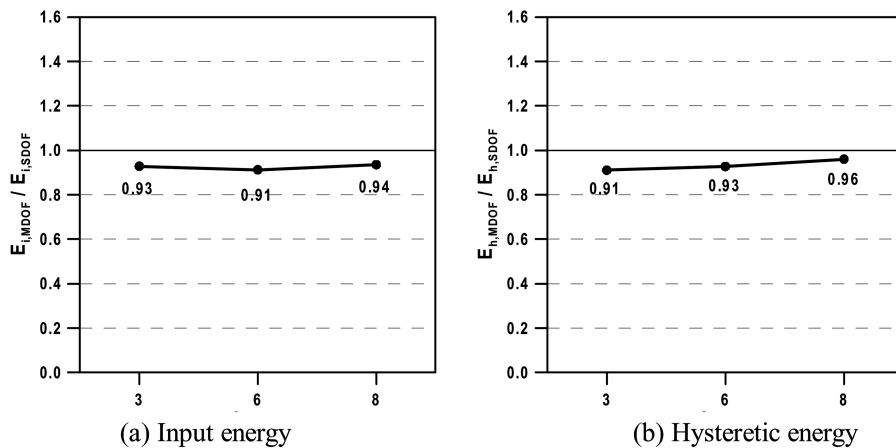

(a) Input energy   (b) Hysteretic energy

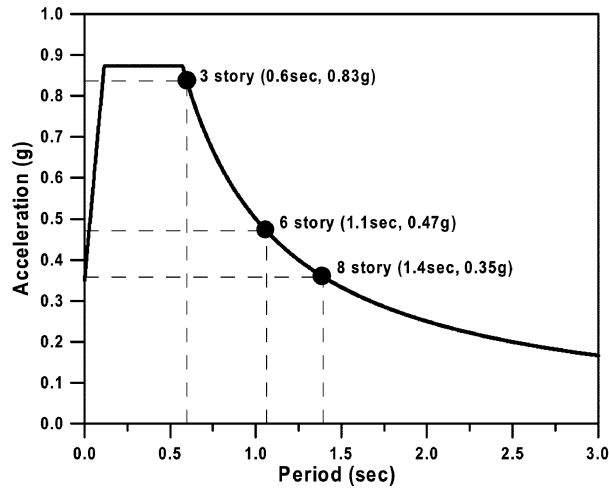Fig. 10 Mean energy ratios of original and equivalent SDOF structures

Fig. 11 Design spectrum of UBC-97 (C_a=0.35 and C_v=0.5)

Fig. 10 presents the ratios of the input and hysteretic energy computed in the original structures and their equivalent SDOF structures. Mean values of 20 analysis results using the earthquakes recorded in soft rock sites were plotted, and were used in the design procedure as modification factors for the use of equivalent SDOF systems.

5.3. Design of BRB to meet a target displacement

The proposed design procedure was applied to the model structures to determine appropriate size of BRB to meet a given target displacement. The target displacements were set to be 1.5% of the structure heights in all model structures. The design spectrum presented in UBC-97 with the seismic coefficients C_a=0.35 and C_v=0.5, as shown in Fig. 11, was used in the design of BRB; the input seismic energy and the hysteretic energy demand were computed from the design spectrum using Eqs. (3) and (4), respectively. The story-wise distribution patterns for hysteretic energy demand obtained in the previous section were applied in the design process. Table 3 presents the design parameters of the 3-story model structure obtained in each iteration step, and Table 4 shows the final values for cross-sectional area of BRB in each story of the model structures. Fig. 12 depicts the fundamental mode shapes of the model structures designed in accordance with the proposed design procedure, where it can be observed that the fundamental mode shape of a structure with BRB is close to a linear line.

Table 3 Design parameters determined in each trial

	1st trial	2nd trial	…	5th trial
T (sec)	0.495	0.689	…	0.597
Sa (g)	0.873	0.726	…	0.838
Total brace area (cm²)	141.7	184.6	…	190.3

Table 4 Cross-sectional area of BRB designed in accordance with the proposed method (unit: cm^2)

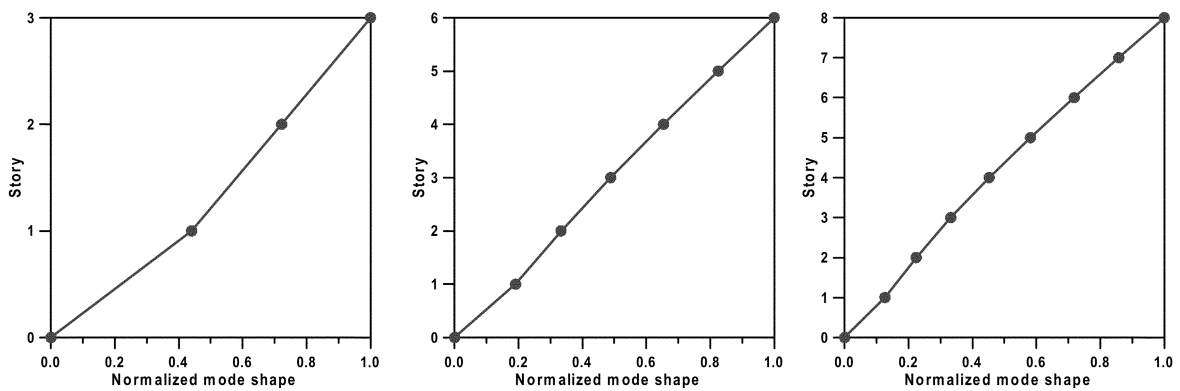| Story	3-story	6-story	8-story
8	-	-	54.8
7	-	-	57.4
6	-	43.4	46.4
5	-	44.5	38.2
4	-	41.4	41.3
3	48.3	48.2	56.0
2	65.7	71.5	81.1
1	76.3	108.6	116.1

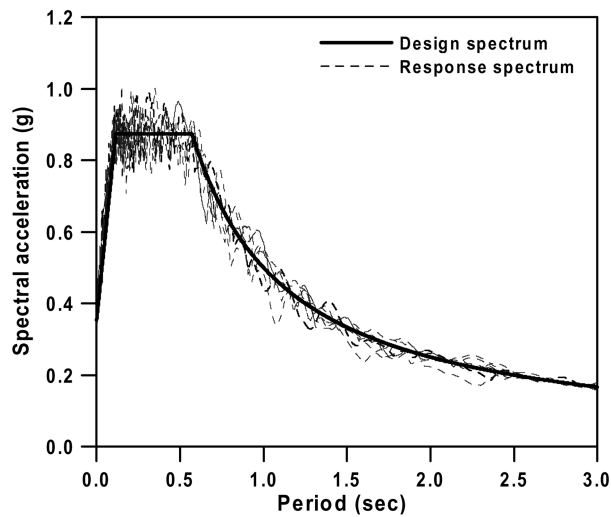Fig. 12 Mode shapes of the model structures

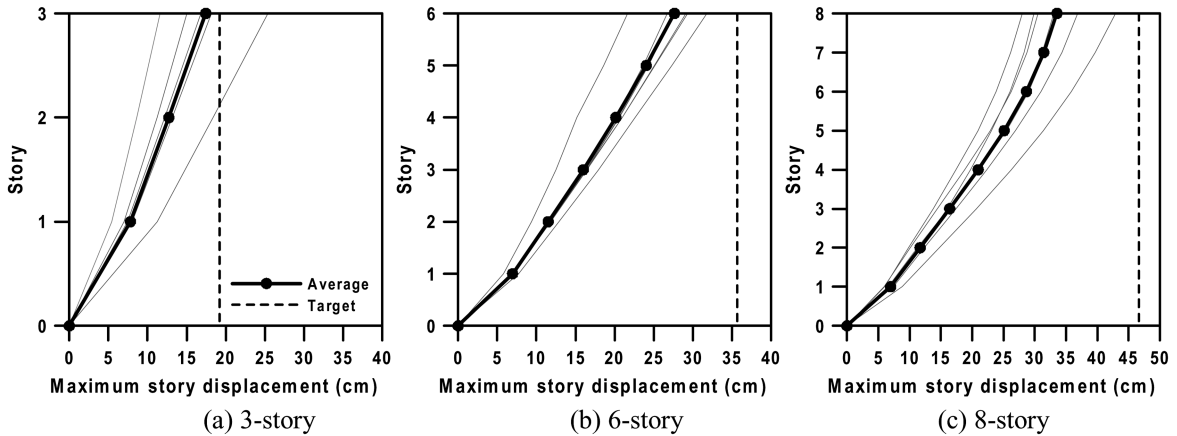Fig. 13 Design spectrum and response spectra of artificial earthquake records

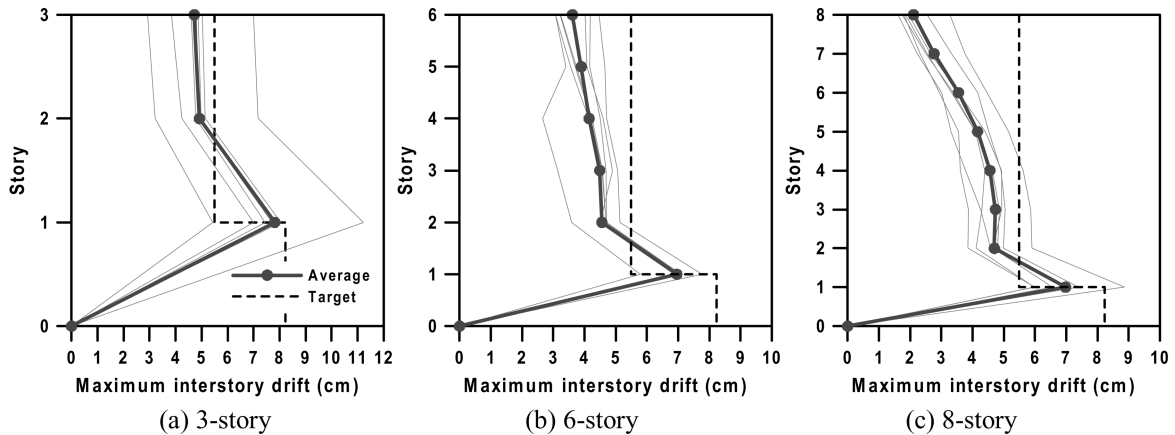Fig. 14. Maximum story displacements obtained from time-history analyses

Fig. 15 Maximum inter-story drifts of the model structures

5.4. Validation of the design using time-history analysis

Seven artificial earthquake records were generated from the design spectrum using the program code SIMQKE (Vanmarcke and Gasparini 1976) to verify the validity of the design procedure through time-history analysis. In Fig. 13 the design spectrum is compared with the response spectrum constructed from the earthquake time-history record, where it can be seen that the response spectrum generally fits well with the original design spectrum. Figs. 14 and 15 depict the maximum story displacements and the maximum inter-story drifts of the model structures obtained from time-history analyses. Mean values of the seven analysis results are plotted in bold lines. According to the analysis results, the maximum story displacements and the maximum inter-story drifts of the 3-story structure generally match with the target displacements on the conservative side. However the results of the 6- and 8-story structures turned out to be somewhat conservative. Therefore based on the analysis results it can be concluded that the seismic design procedure based on the energy balance concept can safely be applied to low-rise structures with BRB. For medium to high-rise structures the procedure may result in too

conservative design. This is reasonable considering the fact that the equal energy concept, in which the total seismic energy stored in a yielding structure is equal to the elastic energy stored in an equivalent elastic structure (Fig. 2), is known to be effective in structures with short natural periods (Leelataviwat *et al.* 2002).

6. Conclusions

In this study a simplified seismic design procedure for structures with buckling-restrained braces was proposed. The validity of the design process as well as the use of equivalent single degree of freedom system was verified through time-history analysis. The story-wise distribution pattern for hysteretic energy demands was also obtained and was applied in the design process.

The analysis results showed that in the 3- and 8-story model structures the energy demands obtained using the equivalent SDOF systems coincided well with those obtained using the original model structures, whereas those in the 20-story structures turned out to be significantly different due to the strong participation of higher modes. It was also observed that the maximum displacement of low-rise structure with BRB designed in accordance with the proposed procedure generally coincides well with the target displacement in 3-and 8-story structures. However the maximum displacements of 6- and 8-story structures turned out to be somewhat lower than the target points, probably due to the participation of higher vibration modes. Therefore it can be concluded that the energy balance concept, which provides simplified procedure for energy-based seismic design, may be safely applicable for seismic design of low-rise structures with BRB.

Acknowledgements

References

Akbas, B., Shen, J. and Hao, H. (2001), "Energy approach in performance-based seismic design of steel moment resisting frames for basic safety objective", *The Structural Design of Tall Buildings*, **10**, 193-217.
ATC (1996), "Seismic evaluation and retrofit of concrete buildings", ATC-40, Applied Technology Council, Redwood City, California.
Black, C., Makris, N. and Aiken, I. (2002), "Component testing, stability analysis and characterization of buckling restrained braces", Final Report to Nippon Steel Corporation, Japan.
Chou, C.C., and Uang, C.M. (2002), "Evaluation of site-specific energy demand for building structures", *Seventh U.S. National Conference on Earthquake Engineering*, Boston, Massachusetts.
Estes, K.R. and Anderson, J.C. (2002), "Hysteretic energy demands in multistory buildings", *Seventh U.S. National Conference on Earthquake Engineering*, Boston, Massachusetts.
Huang, Y.H., Wada, A., Sugihara, H., Narikawa, M., Takeuchi, T., and Iwata, M. (2000), "Seismic performance of moment resistant steel frame with hysteretic damper", *Proc. of the Third Int. Conf. STESSA*, Montreal, Canada.
International code council (2000), 2000 International building code, *Int. Conf. Building Officials*.
Iwata, M., Kato, T. and Wada, A. (2000), "Buckling-restrained braces as hysteretic dampers", *Proc. of Behavior*

of Steel Structures in Seismic Areas, Balkema, Rotterdam.

Leelataviwat, S., Goel, S.C. and Stojadinovic, B. (2002), "Energy-based seismic design of structures using yield mechanism and target drift", *J. Struct. Eng.*, **128**(8), 1046-1054.

Léger, P. and Dussault, S. (1992), "Seismic-energy dissipation in MDOF structures", *J. Struct. Eng.*, **118**(5), 1251-1269.

Riddell, R. and Garcia, J.E. (2001), "Hysteretic energy spectrum and damage control", *Earthq. Eng. Struct. Dyn.*, **30**(12), 1791-1816.

Saeki, E., Maeda, Y., Nakamura, H., Midorikawa, M., and Wada, A. (1995), "Experimental study on practical-scale unbonded braces", *J. Struct. Construct. Eng.*, **476**, 149-158.

SEAOC (2001), "Recommend provisions for buckling-restrained braced frames", in draft form, Structural Engineers Association of California, Sacramento, CA.

Somerville, P., Smith, H., Puriyamurthala, S. and Sun, J. (1997), "Development of ground motion time histories for phase 2 of the FEMA/SAC steel project", SAC Joint Venture, SAC/BD-97/04.

Tremblay, R., Degrange, D. and Blouin, J. (1999), "Seismic rehabilitation of a four-story building with a stiffened bracing system", *Proc. of the 8th Canadian Conf. on Earthquake Engineering*, Vancouver, 549-554.

Tsai, K.C. and Li, J.W. (1997), "DRAIN2D+, A general purpose computer program for static and dynamic analyses of inelastic 2D structures supplemented with a graphic processor", Report No. CEER/R86-07, National Taiwan University, Taipei, Taiwan.

Uang, C.M. and Bertero, V.V. (1988), "Use of energy as a design criterion in earthquake-resistant design", Report No. UCB/EERC-88/18, Earthquake Engineering Research Center, University of California at Berkeley.

Vanmarcke, E.H. and Gasparini, D.A. (1976), "A program for artificial motion generation, user's manual and documentation", Department of Civil Engineering, Massachusetts Institute of Technology.

Yamaguchi, M., *et al.*, (2000), "Earthquake resistant performance of moment resistant steel frames with damper", *Proc. of Behavior of Steel Structures in Seismic Areas*, Balkema, Rotterdam.

CC